

NJC

Accepted Manuscript



This is an *Accepted Manuscript*, which has been through the Royal Society of Chemistry peer review process and has been accepted for publication.

Accepted Manuscripts are published online shortly after acceptance, before technical editing, formatting and proof reading. Using this free service, authors can make their results available to the community, in citable form, before we publish the edited article. We will replace this *Accepted Manuscript* with the edited and formatted *Advance Article* as soon as it is available.

You can find more information about *Accepted Manuscripts* in the [Information for Authors](#).

Please note that technical editing may introduce minor changes to the text and/or graphics, which may alter content. The journal's standard [Terms & Conditions](#) and the [Ethical guidelines](#) still apply. In no event shall the Royal Society of Chemistry be held responsible for any errors or omissions in this *Accepted Manuscript* or any consequences arising from the use of any information it contains.



www.rsc.org/njc

Enhanced water stability and CO₂ gas sorption properties in a methyl functionalized titanium metal-organic framework†

Cite this: DOI: 10.1039/c3nj00000x

Received 00th XXXXX 2013,
Accepted 00th XXXXX 2013

Ji Hyuk Im,^a Nakeun Ko,^b Seung Jae Yang,^a Hye Jeong Park,^b Jaheon Kim^{*b} and Chong Rae Park^{*a}

DOI: 10.1039/c3nj00000x

www.rsc.org/njc

A methyl-modified metal-organic framework (m-TiBDC) shows significantly enhanced hydrostability than unmodified TiBDC, and thus can maintain almost intact CO₂ gas adsorption capacity even after its immersion in water for 2 h while TiBDC does not.

Metal-organic frameworks (MOFs) are porous crystalline materials with regular arrays of metal ions, or metal clusters and organic linkers. Over the past decade, MOFs have been considered as one of the most promising candidates for potential applications such as gas storage and separation, catalysis, sensing, and drug delivery due to their large specific surface area, controllable pore size, and tunable properties.¹⁻⁸ In particular, CO₂ capture from industrial flue gas has become one of the most important environmental issues in recent years. Since the flue gas has 5-10% of water vapour, the framework stability against water vapour is critical for practical applications.⁹ However, many MOFs, which have been not prepared by hydrothermal reactions, are moisture-sensitive because their metal-oxygen coordination bonds are exposed to attack by water in air.¹⁰⁻¹³ Water molecules can easily access to the metal centres in MOFs and substitute coordinated organic linkers, eventually destructing the regular array of building blocks and removing the porosity in MOFs.

As the hydrostability of MOFs is a great issue and also concerned with their practical applications in a bulk scale, various approaches have been recently explored to enhance the framework stability of MOFs against water.¹⁴⁻²⁴ For instances, composites with carbon or silica materials are known to be effective for that purpose as shown in CNT@MOF-5 hybrid,²⁵

carbon-coated MOF-5,²⁶ or MOF-5 confined in SBA-15.²⁷ MOF-5 itself can become more moisture-resistant when its Zn(II) ions are partially exchanged with other transition metal ions such as Ni(II).^{28,29} Compared to these approaches, the modification of organic linkers can take advantages in controlling both the hydrostability and porosity of MOFs in a systematic way. For examples, Cohen and co-workers incorporated a series of hydrophobic alkyl chains onto an amine-containing MOF-5 (IRMOF-3) using the post-synthetic modification method to make the MOF moisture-resistant and even superhydrophobic.²³ Dingemans and co-workers prepared MOF-5-like structures with mono- or dimethyl substituted benzene-1,4-dicarboxylate (BDC) linkers which became water-resistant in a significant extent without impairing the hydrogen uptake capacity.²⁴

Although there have been some promising results on the improving hydrostability of MOFs, it should be noticed that most previous results are focused on the MOFs constructed with Zn(II) as framework metal ions. Herein, we present that a titanium MOF, which is isostructural with MIL-125, can also have improved hydrostability due to the hydrophobic methyl groups introduced in the framework (Fig. 1). Interestingly, the framework structure and CO₂ gas uptake of methyl-functionalized MIL-125 are preserved after water immersion for 2 h.

MIL-125 is the first porous MOF synthesized by using Ti ions as metal ions, and formulated as Ti₈O₈(OH)₄(BDC)₆.³⁰ This MOF has fused eight TiO₆ octahedron units connected by BDC linkers to form a three-dimensional microporous framework. The methyl-modified MIL-125 has been

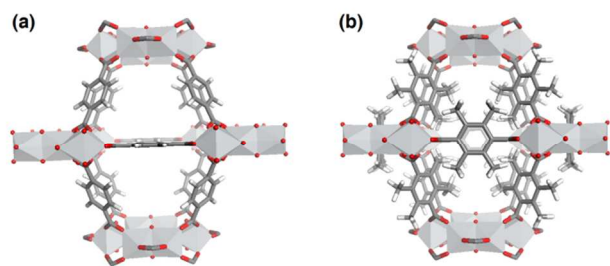


Fig. 1 Fragment structures of (a) TiBDC and (b) m-TiBDC. Color code: Ti, grey; C, grey; O, red; H, white. Ti ions are displayed with octahedron.

synthesized by a solvothermal reaction using a tetramethyl benzene-1,4-dicarboxylic acid ($H_2BDC-Me_4$) as an organic ligand instead of H_2BDC . Unmodified MIL-125 was synthesized for a reference according to the published procedure.³⁰ Hereafter, unmodified and methyl-modified MIL-125 are denoted as TiBDC and m-TiBDC, respectively. The powder X-ray diffraction (PXRD) patterns indicate that the m-TiBDC is analogous to TiBDC in terms of topology, and both measured patterns correspond to the simulated one derived from the optimized model structure of TiBDC (Fig. S1). The molar ratio of ligand to metal is 1:1.3 for m-TiBDC as calculated from thermogravimetric analysis (TGA; Fig. S2), indicating that m-TiBDC has a same metal-to-ligand ratio as in TiBDC. TGA data show that m-TiBDC, which decomposes at 300 °C, has lower thermal stability than TiBDC that is stable until 400 °C.

Structure analyses for the simulated structure of TiBDC and m-TiBDC were conducted by using Materials Studio program³¹ to estimate theoretical accessible surface areas. With fixing the positions of the inorganic clusters $Ti_8O_8(OH)_4(O_2C)_6$, unit cell dimensions, and a space group (Table S1), the geometry of the phenylene moieties were optimized using Molecular Mechanics (MM) calculations. In the case of m-TiBDC, the dihedral angle between the carboxylates groups and phenylene ring was set to 90° similar to the organic linker of IRMOF-18 formulated as $Zn_4O(BDC-Me_4)_3$ (Fig. 1).³² The four methyl groups in BDC- Me_4 give rise to both the increase of framework mass and reduction in the accessibility of a 3.8 Å probe in its diameter, which resulted in a smaller simulated surface area (890 m^2/g) of m-TiBDC than that (2110 m^2/g) of TiBDC. It is clearly shown that the accessible space is much reduced in m-TiBDC, and in addition, the Ti inorganic clusters are almost blocked by the methyl groups protruding into the pores (Fig. 1b).

The N_2 gas sorption isotherms measured at 77 K for TiBDC and m-TiBDC (Fig. S3) show typical Type-I sorption behaviours, suggesting that both materials have the characteristics for the microporosity. The Brunauer–Emmett–Teller (BET) surface areas, micropore volumes, and pore size distribution estimated by using a BJH method for m-TiBDC are compared to those of TiBDC in Table 1. As expected, the BET surface area of m-TiBDC (830 m^2/g) is smaller than that of TiBDC (1550 m^2/g), which is in accordance with the simulated results. In addition, decrease in the micropore volume and pore size of m-TiBDC has been also observed. The CO_2 gas sorption isotherms measured respectively at 253, 273, and 298 K indicate that the CO_2 uptake capacities of m-TiBDC at low pressure region (< 0.2 bar) increase compared with those of TiBDC although the total adsorbed CO_2 amounts up to 1 bar decrease. The isosteric heat (Q_{st}) of CO_2 adsorption (36.65 - 31.87 kJ/mol) in m-TiBDC is higher than that (26.20 - 25.82 kJ/mol) in TiBDC (Fig. S4), as calculated by using a virial

Table 1. Changes in the surface areas and pore volumes of TiBDC and m-TiBDC samples depending on the immersion time in water.

Sample	S_{BET} (m^2/g)	$S_{Langmuir}$ (m^2/g)	V_{total} (cm^3/g)	V_{micro} (cm^3/g)
TiBDC	1550	1700	0.74	0.55
TiBDC_1h	950	1190	0.83	0.29
TiBDC_2h	280	440	0.37	0.07
TiBDC_4h	140	420	0.30	-
m-TiBDC	830	940	0.40	0.30
m-TiBDC_1h	660	880	0.42	0.26
m-TiBDC_2h	550	690	0.41	0.18
m-TiBDC_4h	490	680	0.39	0.15

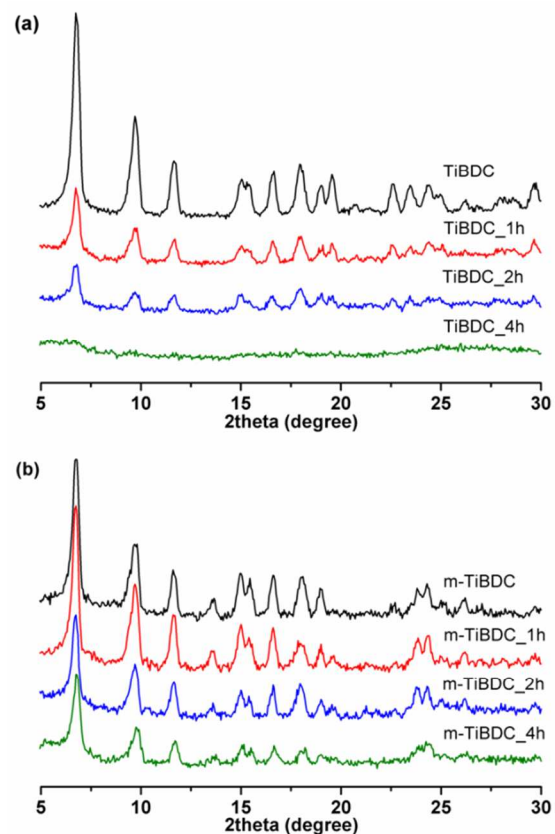


Fig. 2 PXRD patterns of (a) TiBDC and (b) m-TiBDC samples. TiBDC becomes amorphous (TiBDC_4h) while m-TiBDC still keeps crystallinity (m-TiBDC_4h) after water immersion for 4 hours.

fitting.³⁰ The enhanced isosteric heat of CO_2 adsorption might be attributed to the smaller pore size in m-TiBDC, which provides more favourable van der Waals interactions of the framework surfaces with CO_2 molecules.

The water-resistance of two titanium MOFs were compared by measuring the PXRD patterns and gas (N_2 and CO_2) adsorption isotherms of TiBDC and m-TiBDC samples prepared by the immersion in water for 1, 2, and 4 h, respectively. Hereafter, water-treated MOFs are represented as

TiBDC_xh and m-TiBDC_xh (x denotes the immersion time in water). The surface areas and pore volumes of all samples are summarized in Table 1.

As shown in Fig. 2, the diffraction intensity of the original peaks of TiBDC quickly and significantly decreased after 1 h, and the collected sample became amorphous after 4 h, indicating that the framework structure of TiBDC was completely collapsed. In contrast to TiBDC, m-TiBDC showed much enhanced water stability; the sample immersed for 1 h in water produced almost unchanged diffraction peaks, and even the sample immersed in water for 4 h provided significantly strong peaks. This result clearly demonstrates that the introduction of methyl groups to a titanium MOF improves the structural stability against water, which is similar to the observation on the methyl functionalized MOF-5.²⁴

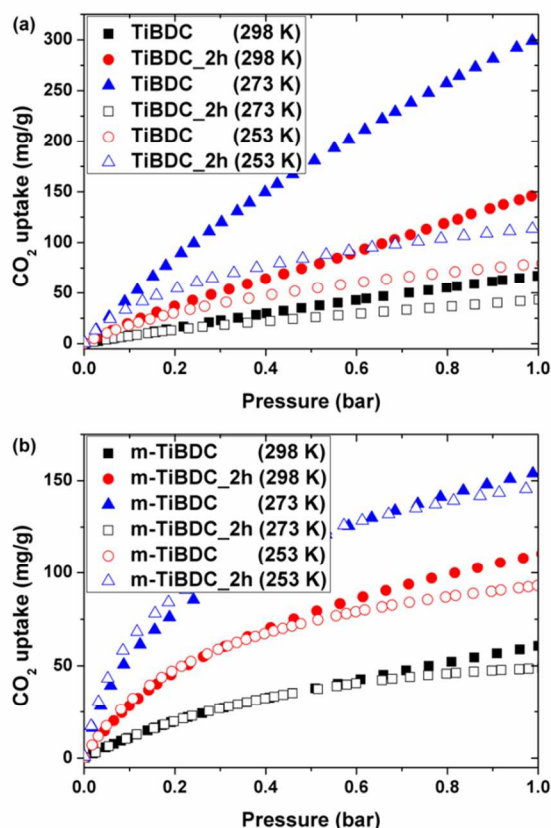


Fig. 3 CO₂ gas sorption isotherms measured at 253, 273, and 298 K, respectively: (a) TiBDC and its water-treated samples (TiBDC_xh) and (b) m-TiBDC and its water-treated samples (m-TiBDC_xh).

The difference in the porosity changes in TiBDC and m-TiBDC were more impressive when the N₂ adsorption isotherms of water-treated samples were analysed. The BET surface area and micropore volume of TiBDC dramatically decrease with increasing immersion time. The water-treated samples of TiBDC lost ca. 90% and 100% in microporosity after 2 and 4 h, respectively, compared to that of pristine TiBDC. However, m-TiBDC showed only lost ca. 40% and 50% in microporosity with the same immersion times, and thus the BET surface area of m-TiBDC_4h was still moderate, 490 m²/g, which corresponds to 59% of the original value of m-TiBDC. Together with the PXRD results, the N₂ adsorption measurements clearly support the contribution of the

hydrophobic methyl groups in organic linkers to marked enhancement of the water stability of m-TiBDC.

CO₂ adsorption isotherms of water-treated samples were measured respectively at 253, 273, and 298 K and pressures up to 1 bar (Fig. 3) to investigate the effect of methyl modification on CO₂ adsorption. As mentioned above, TiBDC showed greater CO₂ uptake than m-TiBDC. However, an opposite result was observed in the samples immersed in water for 2h; after the immersion in water, the CO₂ uptake capacities of TiBDC sharply decreased whereas those of m-TiBDC almost maintained. That is, the CO₂ uptake capacities of m-TiBDC_2h became higher than those of TiBDC_2h at all measured temperatures. This result is not surprising because the BET surface area of m-TiBDC_2h (550 m²/g) is almost twice that of TiBDC_2h (280 m²/g). It is assumed that m-TiBDC_4h would have the same CO₂ adsorption capability as m-TiBDC_2h considering its BET surface area of 490 m²/g. A noticeable point here is not only the absolute amounts of the water-treated samples but the increased water-stability of m-TiBDC; they will be more durable under moisture in flue gas, which is in principle advantageous for practical applications.

In conclusion, we have demonstrated that methyl-modified TiBDC (termed m-TiBDC) exhibits much more excellent water stability than TiBDC. While TiBDC loses almost both the framework structure and porosity after the immersion in water for 4 h, m-TiBDC can maintain its microporous structure as confirmed by PXRD and N₂ gas sorption studies. In addition, m-TiBDC possesses a greater isosteric heat of CO₂ adsorption than TiBDC and its CO₂ adsorption capacity remained almost intact even after water-treatment. In this regard, the introduction of simple hydrophobic functionalities such as methyl groups into the organic linkers is an effective strategy toward the synthesis of a water-stable or moisture-resistant metal-organic framework for practical applications.

Experimental

Synthesis of unmodified MIL-125 (TiBDC)

TiBDC was prepared for a reference by following the literature method.³⁰ Titanium(IV) isopropoxide (Ti(OiPr)₄, Acros Organics, 0.60 mL, 2.0 mmol) and H₂BDC (0.50 g, 3.0 mmol) were put into a mixed solvent system of *N,N*-dimethylformamide (DMF, 9.0 mL) and methanol (1.0 mL). The reaction mixture was then stirred at ambient temperature for 30 min to make a homogeneous solution. The clear solution was transferred to a 23-mL Teflon vessel in a digestion bomb. The reactor was tightly capped and heated at 150 °C for 18 h yielding a white crystalline powder. The solid was filtered and washed with neat DMF (5 × 10 mL) and methanol (3 × 10 mL) before drying under reduced pressure.

Synthesis of methyl-functionalized MIL-125 (m-TiBDC)

Ti(OiPr)₄ (Acros Organics, 0.3 mL, 1.0 mmol) and H₂BDC-Me₄ (0.99 g, 4.5 mmol) were put in a mixed solvent system of DMF (45 mL) and methanol (5 mL). The reaction mixture was then transferred to a 300-mL Teflon vessel in a digestion bomb. The reactor was tightly capped and heated at 150 °C for 18 h yielding a dark-yellow crystalline powder. The solid was filtered and washed with neat DMF (5 × 10 mL) and methanol (3 × 10 mL) before drying under reduced pressure.

Characterization

Powder X-ray diffraction (PXRD) patterns were measured on a Rigaku Miniflex diffractometer with $\text{CuK}\alpha$ ($\lambda = 1.5418 \text{ \AA}$) radiation. Thermogravimetric analyses (TGA) were performed on a TA SDT Q600 with a temperature change of $10 \text{ }^\circ\text{C}/\text{min}$. Nitrogen and carbon dioxide adsorption isotherms were measured on an ASAP 2020 (Micrometrics, USA). Before measurements, the samples were activated at $180 \text{ }^\circ\text{C}$ for 12 h. Specific surface areas were calculated according to the Brunauer–Emmett–Teller (BET) equation with N_2 isotherm points under $P/P_0 < \text{ca. } 0.1$.

Structure Modeling

The optimized structural models of TiBDC and m-TiBDC were built using Materials Studio (Accelrys Inc.).³¹ The known crystal structure of MIL-125³⁰ after generating hydrogen atoms in BDC was subject to Forcite geometry optimization calculations with fixing the positions of Ti and O atoms (except for the O atom in BDC), the unit cell parameters, and the space group. Into the optimized TiBDC model structure, the phenylene rings with generated methyl groups were rotated to 90 degrees to the carboxylate planes in BDC-Me₄. The symmetry of the space group required that two independent BDC-Me₄ linkers should sit on mirror planes. They were modelled not to involve structural disorder or bad contacts between methyl hydrogen atoms. The geometry of the resulting model structure of m-TiBDC was optimized with a same manner as that in TiBDC using the Molecular Mechanics calculations of a Forcite routine. The final atomic coordinates for the structures are listed in Table S1.

Acknowledgements

This research was supported by a grant from the Fundamental R&D Program for Core Technology of Materials funded by the Ministry of Knowledge Economy, Republic of Korea (C.R.P.), and the Korea CCS R&D Center (KCRC) grant funded by the Korea government (Ministry of Science, ICT & Future Planning) (NRF-2012-0008900) (J.K.). We also thank Accelrys Korea for the Forcite calculations of the structures in this work.

Notes and references

^a Carbon Nanomaterials Design Laboratory, Global Research Laboratory, Research Institute of Advanced Materials, and Department of Materials Science and Engineering, Seoul National University, Seoul 151-744, Korea. Fax: +82 2 885 1748; Tel: +82 2 880 8030; E-mail: crpark@snu.ac.kr

^b Institute for Integrative Basic Sciences and Department of Chemistry, Soongsil University, Seoul 156-743, Korea. Fax: +82 2 824 4383; Tel: +82 2 820 0459; E-mail: jaheon@ssu.ac.kr

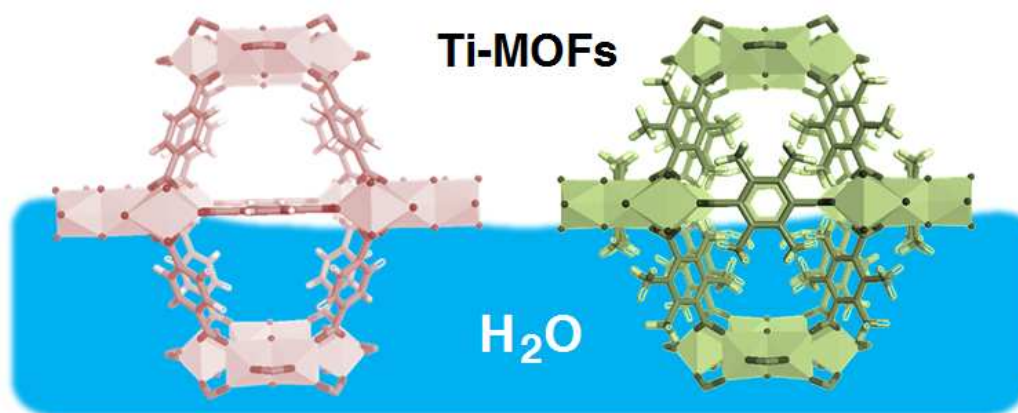
† Electronic Supplementary Information (ESI) available: PXRD patterns, TGA curves, and simulated structures of TiBDC and m-TiBDC, and additional gas sorption data. See DOI: 10.1039/c000000x/

1 S. Kitagawa, R. Kitaura and S. I. Noro, *Angew. Chem. Int. Ed.*, 2004, **43**, 2334.

2 O. M. Yaghi, M. O'Keeffe, N. W. Ockwig, H. K. Chae, M. Eddaoudi and J. Kim, *Nature*, 2003, **423**, 705.

- 3 M. Eddaoudi, J. Kim, N. Rosi, D. Vodak, J. Wachter, M. O'Keeffe and O. M. Yaghi, *Science*, 2002, **295**, 469.
- 4 M. P. Suh, H. J. Park, T. K. Prasad and D.-W. Lim, *Chem. Rev.*, 2012, **112**, 782.
- 5 T. A. Makal, J.-R. Li, W. Lua and H.-C. Zhou, *Chem. Soc. Rev.*, 2012, **41**, 7761.
- 6 C. Wang, D. Liu and W. Lin, *J. Am. Chem. Soc.*, 2013, **135**, 13222.
- 7 A. C. McKinlay, R. E. Morris, P. Horcajada, G. Férey, R. Gref, P. Couvreur and C. Serre, *Angew. Chem. Int. Ed.*, 2010, **49**, 6260.
- 8 A. A. Talin, A. Centrone, A. C. Ford, M. E. Foster, V. Stavila, P. Haney, R. A. Kinney, V. Szalai, F. E. Gabaly, H. P. Yoon, F. Léonard and M. D. Allendorf, *Science*, 2014, **343**, 66.
- 9 K. Sumida, D. L. Rogow, J. A. Mason, T. M. McDonald, E. D. Bloch, Z. R. Herm, T.-H. Bae and J. R. Long, *Chem. Rev.*, 2012, **112**, 724.
- 10 J. J. Low, A. I. Benin, P. Jakubczak, J. F. Abrahamian, S. A. Faheem and R. R. Willis, *J. Am. Chem. Soc.*, 2009, **131**, 15834.
- 11 J. A. Greathouse and M. D. Allendorf, *J. Am. Chem. Soc.*, 2006, **128**, 10678.
- 12 S. S. Kaye, A. Dailly, O. M. Yaghi and J. R. Long, *J. Am. Chem. Soc.*, 2007, **129**, 14176.
- 13 Y. Li and R. T. Yang, *Langmuir*, 2007, **23**, 12937.
- 14 M. H. Weston, A. A. Delaquil, A. A. Sarjeant, O. K. Farha, J. T. Hupp and S. T. Nguyen, *Cryst. Growth Des.*, 2013, **13**, 2938.
- 15 H. Jasuja, N. C. Burtch, Y. Huang, Y. Cai and K. S. Walton, *Langmuir*, 2013, **29**, 633.
- 16 H. Jasuja, Y. Huang and K. S. Walton, *Langmuir*, 2012, **28**, 16874.
- 17 C. R. Wade, T. Corrales-Sanchez, T. C. Narayan and M. Dinca, *Energy Environ. Sci.*, 2013, **6**, 2172.
- 18 L. Bellarosa, J. J. Gutierrez-Sevillano, S. Calero and N. Lopez, *Phys. Chem. Chem. Phys.*, 2013, **15**, 17696.
- 19 H. Jasuja and K. S. Walton, *Dalton Trans.*, 2013, **42**, 15421.
- 20 J. M. Taylor, R. Vaidhyanathan, S. S. Iremonger and G. K. H. Shimizu, *J. Am. Chem. Soc.*, 2012, **134**, 14338.
- 21 Y. Yoo, V. Varela-Guerrero and H.-K. Jeong, *Langmuir*, 2011, **27**, 2652.
- 22 T. Wu, L. Shen, M. Luebbers, C. Hu, Q. Chen, Z. Ni and R. I. Masel, *Chem. Commun.*, 2010, **46**, 6120.
- 23 J. G. Nguyen and S. M. Cohen, *J. Am. Chem. Soc.*, 2010, **132**, 4560.
- 24 J. Yang, A. Grzech, F. M. Mulder and T. J. Dingemans, *Chem. Commun.* 2011, **47**, 5244.
- 25 S. J. Yang, J. Y. Choi, H. K. Chae, J. H. Cho, K. S. Nahm and C. R. Park, *Chem. Mater.*, 2009, **21**, 1893.
- 26 S. J. Yang and C. R. Park, *Adv. Mater.*, 2012, **24**, 4010.
- 27 C.-M. Wu, M. Rathi, S. P. Ahrenkiel, R. T. Koodali and Z. Wang, *Chem. Commun.*, 2013, **49**, 1223.
- 28 H. Li, W. Shi, K. Zhao, H. Li, Y. Bing and P. Cheng, *Inorg. Chem.*, 2012, **51**, 9200.
- 29 C. K. Brozek and M. Dinca, *Chem. Sci.*, 2012, **3**, 2110.
- 30 M. Dan-Hardi, C. Serre, T. Frot, L. Rozes, G. Maurin, C. Sanchez and G. Férey, *J. Am. Chem. Soc.*, 2009, **131**, 10857.
- 31 Materials Studio v6.1, Accelrys Inc., San Diego, CA, 2012.
- 32 J. L. C. Rowsell, A. R. Millward, K. S. Park and O. M. Yaghi, *J. Am. Chem. Soc.*, 2004, **126**, 5666.

Graphic Abstract



A methyl-modified metal-organic framework (m-TiBDC) exhibiting significantly enhanced hydrostability than unmodified TiBDC maintains its framework structure and also CO_2 gas adsorption capacity even after its immersion in water for 2 hours.